

## **Ionized Gas towards Galactic Centre—Constraints from Low-Frequency Recombination Lines**

K. R. Anantharamaiah\**Raman Research Institute, Bangalore 560080*

D. Bhattacharya *Joint Astronomy Program, Department of Physics,  
Indian Institute of Science, Bangalore 560012*

Received 1986 March 7; accepted 1986 April 24

**Abstract.** Observations of the H272 $\alpha$  recombination line towards the galactic centre show features near  $V_{\text{LSR}} = 0, -50$  and  $+36 \text{ km s}^{-1}$ . We have combined the parameters of these features with the available H166 $\alpha$  measurements to obtain the properties of the ionized gas present along the line of sight and also in the ‘3 kpc arm’. For the line-of-sight ionized gas we get an electron density around  $7 \text{ cm}^{-3}$  and a pathlength through it  $\sim 10\text{--}60 \text{ pc}$ . The emission measure and the electron temperature are in the range  $500\text{--}2900 \text{ pc cm}^{-6}$  and  $2000\text{--}6000 \text{ K}$  respectively. The ionized gas in the 3 kpc arm has an electron density of  $30 \text{ cm}^{-3}$  and extends over 9 pc along the line of sight if we assume an electron temperature of  $10^4 \text{ K}$ .

Using the available upper limit to the intensity of the H351 $\alpha$  recombination line, we show that the distributed ionized gas responsible for the dispersion of pulsar signals should have a temperature  $> 4500 \text{ K}$  and a minimum filling factor of 20 per cent. We also show that recombination lines from the ‘warm ionized’ gas proposed by McKee & Ostriker (1977) should be detectable in the frequency range  $100\text{--}150 \text{ MHz}$  towards the galactic centre with the sensitivity available at present.

*Key words:* galactic centre, recombination lines—Galaxy, 3 kpc arm—interstellar medium, distributed ionized gas

### **1. Introduction**

Recombination lines in the direction of the galactic centre have been detected over a wide range of frequencies from 23 GHz (Rodriguez & Chaisson 1979) to 242 MHz (Casse & Shaver 1977). The high-frequency ( $> 5 \text{ GHz}$ ) lines are broad (width  $> 200 \text{ km s}^{-1}$ ) and dominated by emission from high-density gas close to the galactic centre. At lower frequencies a narrow ( $\sim 30 \text{ km s}^{-1}$ ) line near  $0 \text{ km s}^{-1}$  is dominant and is believed to originate in low-density gas along the line of sight (Pedlar *et al.* 1978).

The low-frequency ( $< 500 \text{ MHz}$ ) lines are particularly interesting as they have provided direct evidence for stimulated emission of recombination lines (Pedlar *et al.* 1978). The presence of a strong background continuum source, a long pathlength with no effect of differential galactic rotation, and the dominance of stimulated emission of

\* Present address: National Radio Astronomy Observatory, VLA, P. O. Box 0, Socorro, New Mexico 87801, USA

recombination lines from low-density gas makes this an ideal direction to investigate the properties of any distributed ionized gas in the interstellar medium.

In this paper we make use of the recent H272 $\alpha$  observations (Anantharamaiah 1985a, Paper I) together with the H166 $\alpha$  observations of Kesteven & Pedlar (1977) to derive the properties of the ionized gas along the line of sight to the galactic centre and in the 3 kpc arm. Further, using the upper limit for the H351 $\alpha$  line reported by Hart & Pedlar (1980), we obtain significant constraints on the properties of the distributed ionized gas in the ISM which is responsible for the dispersion of pulsar signals.

## 2. Observations

The H272 $\alpha$  data used in this paper were obtained during the recent survey of recombination lines from the galactic plane at 325 MHz (Paper I) using the Ooty radio telescope (ORT). The strongest recombination line below 500 MHz yet known is towards the galactic centre. This direction was therefore frequently observed during the survey to monitor the functioning of the system. The observing procedure is described in Paper I. A total of 34.5 hours of data were accumulated at the H271 $\alpha$  frequency (328.5958 MHz) using the 64-channel autocorrelator with a total bandwidth of 500 kHz. Independent 62.5 hours of data were accumulated at the H272 $\alpha$  frequency (324.9915 MHz) after the autocorrelator was expanded to 128 channels. The two resulting spectra are shown in Fig. 1. Both these spectra were taken using the full ORT which has an angular resolution of  $2^\circ$  in RA and  $5.6 \text{ sec } \delta \text{ arcmin}$  in declination. A third spectrum was taken using a part of the ORT with an angular resolution of  $2^\circ \times 1^\circ$ . This spectrum which has an integration of 18.6 hours is shown in Fig. 1(d). For comparison we have included in Fig. 1 the H166 $\alpha$  spectrum observed by Kesteven & Pedlar (1977).

It is clear from Figs 1 (b) and (c) that the spectrum taken with an angular resolution of  $2^\circ \times 6.4 \text{ arcmin}$  contains at least four components. They are near velocities of  $-150$ ,  $-50$ ,  $0$  and  $+36 \text{ kms}^{-1}$ . On the other hand, in the spectrum taken with  $2^\circ \times 1^\circ$  resolution (Fig. 1d), it is only the component near  $0 \text{ km s}^{-1}$  which stands out. The other components have weakened below detection limit due to beam dilution.

The parameters of the four components in Fig. 1(b) and one component in Fig. 1(d) obtained from a Gaussian fit are given in Table 1. From what is known about the direction of the galactic centre (*cf.* Radhakrishnan & Sarma 1980) the feature near  $0 \text{ km s}^{-1}$  is due to gas present anywhere along the line of sight. The  $-50 \text{ km s}^{-1}$  feature corresponds to the '3-kpc arm' and the  $+36 \text{ kms}^{-1}$  feature to some gas which is present within 4 kpc from the galactic centre.

The  $-150 \text{ km s}^{-1}$  feature agrees in frequency with the recombination line of carbon or heavier elements, arising anywhere along the line of sight. This feature has a peak  $T_L$  of  $\sim 0.4$  that of the H272 $\alpha$   $0 \text{ kms}^{-1}$  component in the spectrum taken with  $2^\circ \times 6.4 \text{ arcmin}$  resolution. However at lower resolution (Fig. 1d) it is not detected, the  $3\sigma$  upper limit being  $\sim 0.25 T_{L,H272\alpha}$ . This suggests that the angular extent of the region producing this feature must be much smaller than that which produces the H272 $\alpha$  line.

## 3. Ionized gas along the line of sight

Properties of the ionized gas along the line of sight responsible for the low-frequency recombination line near  $0 \text{ km s}^{-1}$  have been discussed by Pedlar *et al.* (1978), Casse &

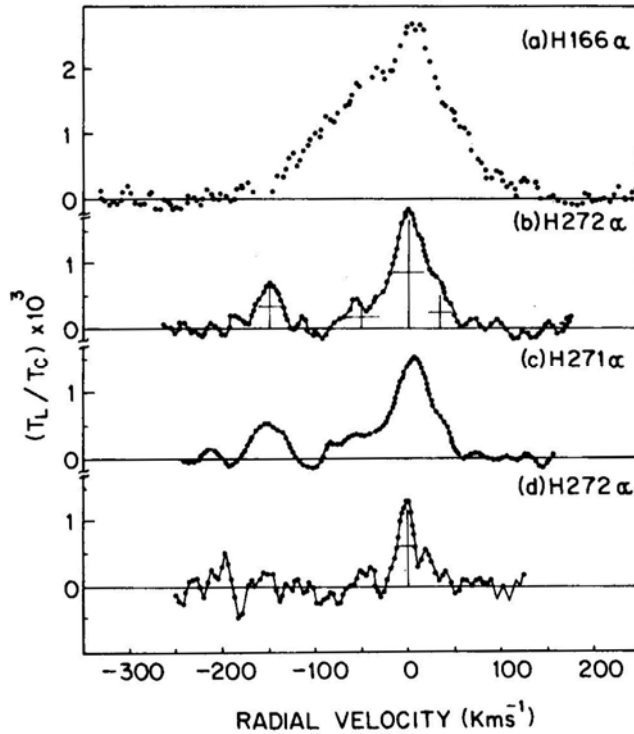


**Figure 1.** Recombination line spectra towards the galactic centre. The H166 $\alpha$  spectrum is from Kesteven & Pedlar (1977). The spectra in (b) and (c) are obtained using the full Ooty radio telescope (ORT) which has an angular resolution of  $2^\circ \times 6.4$  arcmin. The H272 $\alpha$  line observed using a part of the ORT (resolution  $2^\circ \times 1^\circ$ ) is shown in (d). The crosses indicate the fitted gaussian components.

Shaver (1977) and Hart & Pedlar (1980). Although line emission near  $0 \text{ km s}^{-1}$  can accumulate over a long pathlength in this direction, it has been shown that the observed lines can be explained in terms of a single low-density, low-emission-measure, extended H II region (Pedlar *et al.* 1978) or two overlapping H II regions (Hart & Pedlar 1980) in the line of sight to the galactic centre.

Higher-frequency recombination lines at several positions around the galactic centre have been observed by Lockman & Gordon (1973), Pauls *et al.* (1976) and Kesteven &

**Table 1.** 272 $\alpha$  line parameters.

Beam	Line	$V_{\text{LSR}} \text{ km s}^{-1}$	$\Delta V \text{ km s}^{-1}$	$T_L/T_C \times 10^3$	$T_L^\dagger (\text{k})$	$T_C^\dagger (\text{k})$
$2^\circ \times 6'.4$	H272 $\alpha$	$2.1 \pm 0.5$	$37 \pm 1$	$1.7 \pm 0.05$	$4.0 \pm 0.1$	2330
		$-49 \pm 2$	$38 \pm 5$	$0.4 \pm 0.05$	$0.93 \pm 0.12$	
		$36 \pm 1$	$24 \pm 3$	$0.5 \pm 0.06$	$1.2 \pm 0.1$	
$2^\circ \times 1^\circ$	C272 $\alpha$	$-149.5 \pm 1$	$26 \pm 2$	$0.7 \pm 0.06$	$1.6 \pm 0.1$	
	H272 $\alpha$	$0.5 \pm 1$	$15 \pm 2$	$1.2 \pm 0.1$	...	...

$\dagger$  Beam averaged brightness temperature.  
Errors quoted are  $1\sigma$  values.

Pedlar (1977). As discussed by Anantharamaiah (1985b, Paper II) it is possible to derive the electron density in the gas irrespective of its temperature if both high-frequency ( $> 1$  GHz) and low-frequency ( $< 500$  MHz) recombination lines are observed from the same gas. This is because the intensity of recombination lines at high frequencies is dominated by spontaneous emission and at low frequencies by stimulated emission. As a result the two intensities have a very different dependence on the electron density.

The excess temperature produced at the frequency of the recombination line by a homogeneous ionized region located in front of a background continuum source is given by (Shaver 1975a)

$$\begin{aligned}
 T_L = T_0 [e^{-\tau_c} (e^{-\tau_L} - 1)] \\
 + T_e \left[ \frac{b_m \tau_L^* + \tau_c}{\tau_L + \tau_c} (1 - e^{-(\tau_L + \tau_c)}) - (1 - e^{-\tau_c}) \right] \\
 + T_M \left[ \frac{1 - e^{-(\tau_L + \tau_c)}}{\tau_L + \tau_c} - \frac{1 - e^{-\tau_c}}{\tau_c} \right] \quad (1)
 \end{aligned}$$

where  $T_0$  is the continuum temperature of the background source,  $T_e$  the electron temperature of the ionized region and  $T_M$  represents the nonthermal background distributed inside this region.  $\tau_c$  and  $\tau_L$  are the continuum and line optical depths respectively.  $\tau_L^*$  is the line optical depth in LTE. The expressions for these are given in Oster (1961) and Shaver (1975a). The coefficients  $b_m$  giving the ratio of the true and LTE populations were calculated using the computer code published by Brocklehurst & Salem (1977). We have modified this code to incorporate the effect of the galactic nonthermal background on the level populations. A radiation temperature  $T_R = 400$  K at 408 MHz and a spectral index  $\alpha = -0.7$  (Intensity  $\propto \nu^\alpha$ ) was used in the calculations.

The angular extent of the region which produces the emission near  $0 \text{ km s}^{-1}$  is estimated to be greater than  $1^\circ$  (Kesteven & Pedlar 1977) and may be as large as  $2^\circ.5$  (Hart & Pedlar 1980). Therefore the H166 $\alpha$  measurements of Kesteven & Pedlar (1977) (beam size  $12 \text{ arcmin} \times 12 \text{ arcmin}$ ) do not suffer from beam dilution. On the other hand, the H272 $\alpha$  measurements reported here are made with a  $2^\circ \times 6.4 \text{ arcmin}$  beam and therefore a dilution factor may have to be taken into account while using Equation (1).

The H166 $\alpha$  line in the direction ( $l = 0, b = 0$ ) can have a large contribution from stimulated emission due to the strong background source in that direction. In addition there will also be a contribution from higher-density gas present close to the galactic centre (Pauls *et al.* 1974). To minimize such complications we use the H166 $\alpha$  measurement at ( $l = 0, b = +0.4$ ) where the 1.4 GHz continuum temperature is a minimum (Kesteven & Pedlar 1977). Also there is no discrete source in this direction in the 5 GHz high-resolution map of Altenhoff *et al.* (1978), precluding the presence of a discrete dense HII region capable of making significant contribution to H166 $\alpha$  emission. The H166 $\alpha$  line parameters observed at this position are  $T_{L\text{max}} = 0.14 \pm 0.04$  K and  $T_c = 34 \pm 5$  K. The H272 $\alpha$  parameters are given in Table 1.

The combination of emission measure and electron density required to produce the observed intensities of the H166 $\alpha$  and the H272  $\alpha$  lines (near  $0 \text{ km s}^{-1}$ ) is shown in Fig. 2. These calculations were done using Equation (1). We assumed that the region extends  $1^\circ.2$  in RA based on the measurements of Kesteven & Pedlar (1977). This results in a beam dilution factor of 0.6 for the H272 $\alpha$  line. A region with such large angular extent is most likely to be nearby and in front of the dominant source of continuum, namely the

Sagittarius A region. We therefore assumed all of the continuum radiation to originate behind the cloud. If we require that the H166 $\alpha$  and the H272 $\alpha$  lines arise in the same gas then the electron density in the gas is given by the intersection of the two sets of curves in Fig. 2. This gives a density of  $\sim 7 \text{ cm}^{-3}$  and is practically independent of the electron temperature. If the region is larger than  $2^\circ$  in RA (no dilution for the H272 $\alpha$ ) then we get a density of  $16 \text{ cm}^{-3}$  which can be considered as an upper limit. Fig. 3 shows the relation between the temperature and emission measure (and therefore the pathlength) of this gas, taking the electron density to be  $7 \text{ cm}^{-3}$ . A lower limit to the pathlength through this gas can be set by considering the geometry of the region and an upper limit results from the average interstellar electron density obtained from pulsar dispersion measure (see Paper II). The angular extent of this region is at least  $1^\circ$ . Even if this gas is nearby, say at 2 kpc, its linear extent perpendicular to the line of sight is  $\sim 34 \text{ pc}$ . Therefore to avoid peculiar geometry the line-of-sight extent of this gas is likely to be larger than, say,  $\sim 10 \text{ pc}$ . This implies that  $\text{EM} > 500 \text{ pc cm}^{-6}$  and  $T_e > 2000 \text{ K}$  (Fig. 3). Vivekanand & Narayan (1982) have estimated the contribution to the line-of-sight

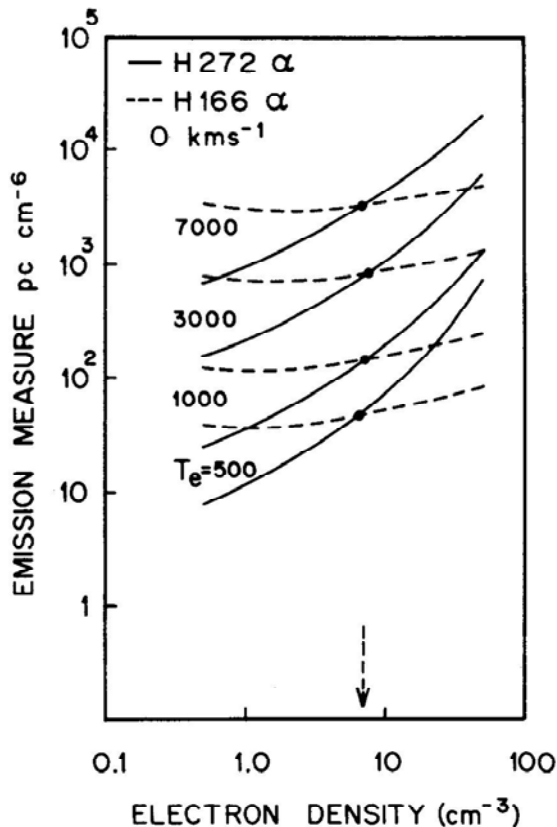


**Figure 2** The relation between emission measure and electron density of the gas required to produce the observed intensity of the H16 (dashed line) and the H272 $\alpha$  lines (full line) near  $0 \text{ km s}^{-1}$ . Curves are shown for different electron temperatures. If the two lines are produced in the same gas then the intersection points (dots) indicate the electron density, which is virtually independent of the temperature.

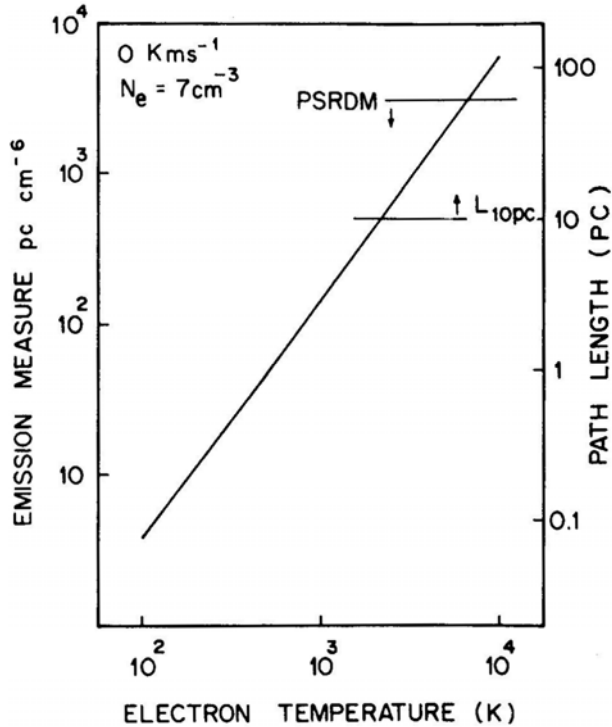


**Figure 3.** Constraints on the electron temperature, emission measure and pathlength through the ionized gas towards the galactic centre. Electron density derived from Fig. 2 has been used. The pathlength marked on the right follows directly from the emission measure and the electron density. The diagonal line represents the constraint based on the observed recombination lines ( $0 \text{ km s}^{-1}$  components). Upper limit to the pathlength comes from consideration of the average interstellar electron density obtained from pulsar dispersion measure (PSRDM). Lower limit is obtained from the geometry of the line-emitting region ( $L_{10\text{pc}}$ ). See text for arguments.

average electron densities from localized higher-density ionized regions (*e.g.* HII regions) to be  $\leq 0.02 \text{ cm}^{-3}$  (see Paper II for a more detailed discussion). This would constrain the pathlength through this gas to less than  $\sim 60 \text{ pc}$ , implying that  $\text{EM} \leq 2900 \text{ pc cm}^{-6}$  and  $T_e \leq 6000 \text{ K}$  (Fig. 3).

The properties deduced above for the line-of-sight ionized gas suggests that it may be a single large evolved HII region. Though more than one HII regions may be present along the line of sight, beam dilution will restrict the detection of line emission from the nearby ones. The parameters obtained in Paper II indicate that the low-density envelope of a single evolved HII region is quite adequate to explain the observed line strengths.

#### 4. Ionized gas in the ‘3 kpc arm’

The feature near  $-50 \text{ km s}^{-1}$  in the H272 $\alpha$  spectra (Fig. 1) can be attributed to ionized gas present in the so called ‘3-kpc arm’ which is believed to be an expanding ring at a distance closer to 4 kpc from the galactic centre. The 3 kpc arm is a prominent feature in

both H $\text{I}$  and CO emission from this region (see for example Cohen & Davies 1976; Bania 1980). It is also seen in H $\text{I}$  absorption in the direction of the galactic centre (e.g. Schwarz, Ekers & Goss 1982).

Emission near  $-50 \text{ km s}^{-1}$  can be clearly seen in the H159 $\alpha$  and the H166 $\alpha$  spectra of Lockman & Gordon (1973) and Kesteven & Pedlar (1977) respectively. The H166 $\alpha$  emission from the 3 kpc arm has been discussed by Lockman (1980).

The detection of the H272 $\alpha$  line indicates that low-density ionized gas is present in the 3 kpc arm. As in the previous section we can determine the electron density of this gas by using both the H272 $\alpha$  and the H166 $\alpha$  measurements.

The measured H272 $\alpha$  line parameters of the  $-50 \text{ km s}^{-1}$  component are given in Table 1. The angular size of the region producing this feature is about 30 arcmin from the high-resolution measurements of H166 $\alpha$  line by Kesteven & Pedlar (1977). This corresponds to a beam dilution factor of 0.25 for the H272 $\alpha$  line. It is interesting to note that if observations are made with higher angular resolution, the H272 $\alpha$  line from the 3 kpc arm would be as strong as the feature near  $0 \text{ km s}^{-1}$ . We estimated the background temperature (in Equation 1) over the  $30 \text{ arcmin} \times 6.4 \text{ arcmin}$  of this region seen by the beam of the ORT by using (i) the measured beam brightness temperature at 325 MHz (Table 1), (ii) the 408 MHz map of the galactic centre region by Little (1974), and (iii) the 408 MHz all sky map of Haslam *et al.* (1982). We get  $T_0 = 5000 \text{ K}$ . We used  $T_M = 0$  since the maximum pathlength through this region is equal to the thickness of the 3 kpc arm ( $\sim 700 \text{ pc}$ , Simonson & Mader 1973).

We chose the H166 $\alpha$  measurement at  $(l, b) = (0, +0.2)$  instead of at  $(0, 0)$  for the reason discussed in the previous section. The measured parameters are  $T_L = 0.15 \text{ K}$  and  $T_C = 90 \text{ K}$  (Kesteven & Pedlar 1977).

With these parameters we get an electron density of  $30 \text{ cm}^{-3}$  using similar calculations as for Fig. 2. The relation between the electron temperature and emission measure (which also gives a pathlength since  $n_e$  is fixed) for the ionized gas in the 3 kpc arm is shown in Fig. 4.

As seen in this figure the pathlength through the gas is 9 pc for an electron temperature of  $10^4 \text{ K}$ . The thickness of the 3 kpc arm is  $\sim 700 \text{ pc}$  (Simonson & Mader 1973). This gives a value of 0.01 for the filling factor along the line of sight for the ionized gas in this arm, suggesting that discrete H $\text{II}$  regions can well account for all of this gas. The column density of electrons in the 3 kpc arm comes out to be  $9.3 \times 10^{19} \text{ cm}^{-2}$ . The ratio of this to the column density of neutral hydrogen (estimated by Radhakrishnan & Sarma (1980):  $N(\text{H}\text{I}) = 1.2 \times 10^{21} \text{ cm}^{-2}$  for  $T_s = 100\text{K}$ ) is 0.08.

## 5. The +36 kins<sup>1</sup> feature

This feature is clearly seen in both the H272 $\alpha$  and H271 $\alpha$  spectra (Figs 1b, c). The presence of a positive velocity feature in the H252 $\alpha$  spectrum towards the galactic centre has been noted by Pedlar *et al.* (1978). This feature is also seen in the H166 $\alpha$  spectrum of Kesteven & Pedlar (1977).

The ionized gas responsible for this component must be lying inside of 4 kpc from the galactic centre where noncircular motions are known to be prevalent. We have not attempted to determine the electron density of this gas since its angular extent cannot be determined from existing observations. The observed width of the H272 $\alpha$  line

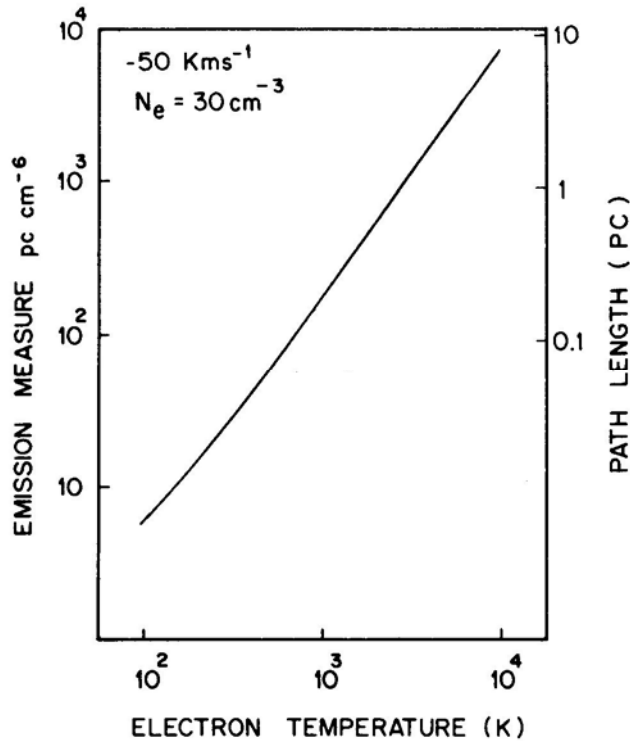


**Figure 4.** Constraints on the electron temperature, emission measure and pathlength through the ionized gas in the '3 kpc arm'. The electron density was obtained from calculations as in Fig. 2 based on the intensity of the H272 $\alpha$  and the H166 $\alpha$  lines near  $-50 \text{ kms}^{-1}$ .

implies an upper limit to the electron density of  $25 \text{ cm}^{-3}$  from considerations of pressure broadening.

## 6. Constraints on the distributed ionized gas in the ISM

The sensitivity of low-frequency recombination lines to conditions in low-density ionized regions make these lines particularly suitable for the study of the distributed ionized component of the interstellar medium. Several attempts have so far been made in this direction (Shaver 1975b, 1976; Shaver, Pedlar & Davies 1976; Hart & Pedlar 1980). Existence of a distributed ionized component of the ISM has been inferred mainly from the dispersion measures of pulsars, which yield a line-of-sight average electron density  $\langle n_e \rangle = 0.03 \text{ cm}^{-3}$  (Falgarone & Lequeux 1973; Gómez-González & Guélin 1974; del Romero & Gómez-González 1981; Harding & Harding 1982; Vivekanand & Narayan 1982 and many others). Other properties of this gas are rather difficult to determine and have remained uncertain to date. It was originally thought to be a uniformly distributed, partially ionized gas with filling factor close to unity (see for example Field, Goldsmith & Habing 1969). However, since then ultraviolet absorption lines of OVI have been seen in the ISM (Rogerson *et al.* 1973; Jenkins & Meloy 1974; York 1974), and the ubiquity of these lines suggest that a fair fraction of the galactic disc

must be filled with hot ( $T \sim 10^6$  K), coronal gas of very low density ( $n \sim 0.003 \text{ cm}^{-3}$ ) (Spitzer 1956; see Jenkins 1984 for a recent review). It has therefore become necessary to modify the old picture of a uniform intercloud medium by introducing ionized clumps with higher density and smaller filling factor, so as to maintain the average electron density required to account for pulsar dispersion measures, as well as to accommodate the coronal gas. For example, in the model of McKee & Ostriker (1977), this ‘warm’ gas has a local electron density  $n_e = 0.17 \text{ cm}^{-3}$  and a filling factor  $f_w = 0.23$ . Nevertheless there is still a considerable controversy regarding these values (e.g. Heiles 1980; see Cowie & Songaila, 1986 for a recent review). As will be clear from the following discussion, low-frequency recombination lines are likely to provide a direct handle on the local densities and temperatures of this ‘warm’ ionized gas. In this section we shall attempt to obtain constraints on the parameters of this warm gas using the presently available upper limit on the H351 $\alpha$  line emission from the direction of the galactic centre (Hart & Pedlar 1980).

The picture adopted for the line-of-sight gas towards the galactic centre is shown in Fig. 5. Clumps containing ionized gas at local density  $n_e$  contribute to the recombination-line emission. The total pathlength  $L$  in this direction is 20 kpc, of which only a fraction  $f_w$  is through the ionized region of interest. Here  $f_w$  is the filling factor defined by  $f_w = \langle n_e \rangle / n_e$ . The emission measure  $\text{EM} = n_e^2 f_w L = n_e \langle n_e \rangle L$ . Since the value of  $\langle n_e \rangle$  is known from pulsar dispersion measure, the local density  $n_e$  directly determines the filling factor and the emission measure. This unique correspondence between  $n_e$  and EM allows one to obtain (using Equation 1) a relation between  $n_e$  and  $T_e$  given that this gas should produce the required line intensity. The appropriate values of  $T_0$  and  $T_M$  are obtained as follows.

Let  $T_N$  be the contribution of the nonthermal galactic background to the total observed continuum temperature  $T_C$ .  $T_{\text{Sgr}} = T_C - T_N$  can then be taken as the beam brightness temperature of the Sagittarius A region, assuming the continuum emission from other discrete sources in the line of sight to be negligible. The total amount of nonthermal background that originates within the clumps is simply  $T_M = f_w T_N$ . The rest of the nonthermal background originates outside the clumps contributing to the background temperature:  $T_0 = T_{\text{Sgr}} + \frac{1}{2} (T_N - T_M)$ . Since the stimulated emission due to  $T_0$  is effective only over half the line of sight (due to the central location of Sgr A), we used half the total pathlength in the first term of Equation (1).

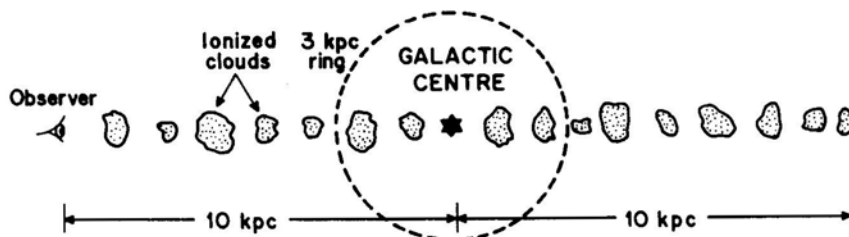


**Figure 5.** A schematic picture of the line of sight towards the galactic centre. The total pathlength through the galaxy is  $\sim 20$  kpc. The distributed ionized component of the interstellar medium, which is responsible for dispersion of pulsar signals, resides in clumps represented as ionized clouds. The strong continuum source at the galactic centre causes stimulated emission of recombination lines from this gas over half the total pathlength through the Galaxy. The clumps inside the 3 kpc ring may have nonzero radial velocity due to noncircular motions.

From the 151 MHz observations reported by Hart & Pedlar (1980) we obtain  $T_C = (20800 \pm 1600)$  K and  $T_{L,351\alpha} < 8$  K after correcting for beam efficiency factors.  $T_L = 8$  K can then be used as an absolute upper limit to the contribution of the warm ionized gas to the H351 $\alpha$  transition. The  $(n_e, T)$  combinations required to produce this line intensity are shown in Fig. 6 (curve b), where  $\langle n_e \rangle = 0.03 \text{ cm}^{-3}$  and  $L = 20$  kpc was used. The fact that  $T_L = 8$  K is an upper limit restricts the parameters of the gas to those above this line. The value of  $n_e$  for this gas, of course, cannot be less than  $0.03 \text{ cm}^{-3}$ , which corresponds to a filling factor  $f_w = 1$ . This sets a lower limit of 4500 K to the temperature  $T$  of this ionized component. An independent restriction on the parameters of this gas comes from the requirement of pressure equilibrium in the ISM. For an average ambient interstellar pressure  $P_0$ , the allowed values of  $n_e$  and  $T$  must be such that  $n_e T \leq \frac{1}{2} P_0 / k$ , where  $k$  is Boltzmann's constant. The equality is reached only in the case of complete ionization. The implicit assumptions here are, of course, that the neutrals, ions and electrons have the same temperature and that most electrons are provided by singly ionized species. Both these assumptions seem reasonable under normal interstellar conditions. We adopt a value of  $P_0 / k = 3200 \text{ cm}^{-3} \text{ K}$ , consistent with the value used by McKee & Ostriker (1977). The line corresponding to  $n_e T = 1600 \text{ cm}^{-3} \text{ K}$  is also shown in Fig. 6. The allowed region of the parameter space lies to the left of this line. The intersection of this line with curve (b) gives an upper limit to the electron density, and hence a lower limit to the filling factor of this gas:  $n_e < 0.2 \text{ cm}^{-3}$ ,  $f_w > 0.15$ . The filled circle in this diagram represents the parameters for the warm ionized medium ( $n_e = 0.17 \text{ cm}^{-3}$ ,  $T = 8000$  K) chosen by McKee & Ostriker (1977). If the actual parameters are indeed close to this value then it is evident from the diagram that with slightly increased sensitivity one should be able to detect low-frequency recombination lines from this gas.

In the above discussion we have attributed the entire  $\sim 8$  K line temperature to that arising from the distributed interstellar gas. However, as the analysis in Section 3 has shown, there is a relatively dense discrete ionized region in the above line of sight, which is also likely to contribute to the H351 $\alpha$  emission. The electron density derived for this region is in the range  $7\text{--}16 \text{ cm}^{-3}$ , the higher values corresponding to smaller beam dilution for the H272 $\alpha$ . If this region is indeed so large that the dilution in the 151 MHz beam ( $2^\circ.5 \times 2^\circ.5$ ) is small, then the corresponding high inferred densities ( $n_e \sim 16 \text{ cm}^{-3}$ ) will pressure broaden the H351 $\alpha$  line to more than  $80 \text{ kms}^{-1}$  and any such contribution would have been removed in the process of baseline subtraction. On the other hand, at lower densities ( $n_e \sim 7 \text{ cm}^{-3}$ ) the region would produce a strong line but in this case the region will be of small angular size, and beam dilution will be appreciable. The maximum contribution to the H351 $\alpha$  line from this dense gas is thus estimated to be  $\sim 3\text{--}5$  K. If we attribute the remaining  $\sim 4$  K to emission from the distributed component, then in Fig. 6 the lower boundary of the allowed region moves up somewhat, as shown by curve (d). This gives  $T > 6000$  K,  $n_e < 0.16 \text{ cm}^{-3}$ ,  $f_w > 0.2$ . Interestingly, the warm ionized medium of McKee & Ostriker (1977) now falls outside the allowed region. It is clear that even a slight improvement in the H351 $\alpha$  upper limit may require the parameters of the warm ionized medium to be modified; lower densities and correspondingly higher filling factor may be necessary.

Uncertainties in the above estimate are introduced by significant noncircular motion of gas within  $\sim 3$  kpc of the galactic centre. This restricts the total pathlength over which line emission can accumulate at zero velocity. If we assume that this central region makes no contribution at all to the line emission, then  $L$  is reduced to 14 kpc,

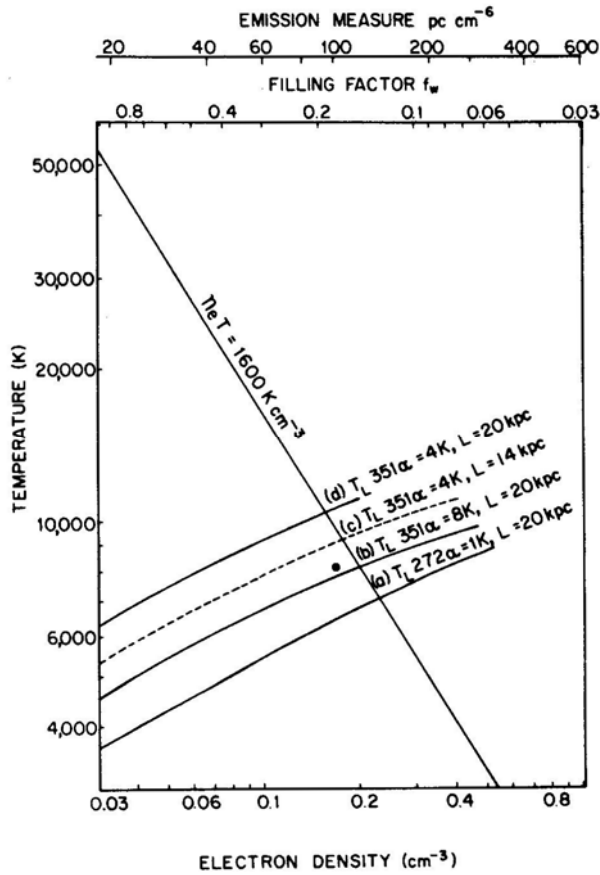


**Figure 6.** Constraints on the temperature ( $T$ ), local electron density ( $n_e$ ) and filling factor ( $f_w$ ) of the distributed ionized gas which has an average electron density  $\langle n_e \rangle = 0.03 \text{ cm}^{-3}$ . The markings on the top are obtained using,  $f_w = \langle n_e \rangle / n_e$  and  $\text{EM} = n_e \langle n_e \rangle L$ , where  $L = 20 \text{ kpc}$ . The constraints are obtained from pressure equilibrium in the ISM (the line marked  $n_e T$ ) and the intensity of the low-frequency recombination lines in the direction of the galactic centre (lines marked a, b, c and d). The strictly allowed parameters for this ionized gas are below the line marked  $n_e T$  and above the line (b) which results from an observed upper limit of 8 K to the H351 $\alpha$  line (Hart & Pedlar 1980). Our realistic estimate of the upper limit to the H351 $\alpha$  line restricts the parameters to above the dashed line (c). The filled circle indicates the parameters of the warm ionized gas in the model of McKee & Ostriker (1977).

which weakens the above-mentioned limits to some extent.  $T_{L351\alpha} = 4\text{K}$  line for  $L=14 \text{ kpc}$  is shown in Fig. 6 (curve c). The change, however, is not more than  $\sim 10$  per cent.

Another factor that has not been included in the above analysis is the absorption by the thermal gas around the galactic centre. This will restrict the amount of line radiation received from behind the galactic centre. We estimate the error due to this to the final result to be small ( $\leq 10$  per cent), since most of the line emission arises in front of the galactic centre, because of stimulated emission due to strong continuum radiation from the galactic centre region.

It appears that frequencies in the range 100–150 MHz are most suitable for the purpose of studying recombination-line emission from distributed ionized component of the ISM. At higher frequencies most of the line emission comes from the localized dense gas in this line of sight, as discussed in Section 3. For example, based on the H351 $\alpha$  upper limit, we estimate the contribution of the distributed component to the H272 $\alpha$  line intensity to be  $< 0.6$  K, whereas the total observed H272 $\alpha$  line intensity is  $\sim 4$  K. We have shown in Fig. 6 (curve a), for purposes of comparison, the line corresponding to  $T_{L,272\alpha} = 1$  K contribution from the distributed gas. Frequencies much lower than 100 MHz, though more sensitive to the low-density component, suffer from the fact that the dense gas mentioned above becomes optically thick, thus drastically reducing the pathlength over which line emission can accumulate. It seems extremely important, therefore, to carry out new observations at 100–150 MHz with improved sensitivity to obtain a direct handle on the properties of the distributed ionized component of the interstellar medium.

## 7. Conclusions

The H272 $\alpha$  recombination line in the direction of the galactic centre is seen at velocities near 0 km s $^{-1}$ ,  $-50$  km s $^{-1}$  and  $+36$  km s $^{-1}$ . These features are also evident in the H166 $\alpha$  observations of Kesteven & Pedlar (1977). The feature near 0 km s $^{-1}$  is due to ionized gas along the line of sight. We attribute the  $-50$  km s $^{-1}$  feature to ionized gas present in the ‘3 kpc arm’ and the  $+36$  km s $^{-1}$  feature to ionized gas inside of 4 kpc from the galactic centre.

The properties of the ionized gas responsible for these features are deduced using a single-component model to fit both the H272 $\alpha$  and the H166 $\alpha$  observations. We obtain an electron density of about 7 cm $^{-3}$  for the ionized gas along the line of sight. From considerations of the geometry of the line-emitting region and the average interstellar electron density, we deduce that the pathlength through this gas is in the range 10–60 pc. This corresponds to a possible range in the emission measure of 500–2900 pc cm $^{-6}$  and in the electron temperature of 2000–6000K.

The electron density derived for the ionized gas in the 3 kpc arm is about 30 cm $^{-3}$ . For an electron temperature of 10 $^4$ K, the pathlength through this gas is 9 pc. This leads to an electron column density of  $9.3 \times 10^{19}$  cm $^{-2}$  and a ratio of electron to neutral hydrogen column density of 0.08.

The upper limit on the H351 $\alpha$  line in the direction of the galactic centre (Hart & Pedlar 1980) imposes strong constraints on the properties of the distributed ionized gas responsible for the dispersion of pulsar signals. We obtain a *lower limit* to its electron temperature (7) of 4500 K. Assuming this gas to be in pressure equilibrium with the ISM, we get an *upper limit* to its electron density ( $n_e$ ) of 0.2 cm $^{-3}$  which corresponds to a *lower limit* to the line-of-sight filling factor ( $f_w$ ) of 0.15. These limits are somewhat conservative. Our more realistic estimates are  $T > 6000$ K,  $n_e < 0.16$  cm $^{-3}$  and  $f_w > 0.2$ . The parameters for the ‘warm ionized’ component of the ISM proposed by McKee & Ostriker (1977) are only marginally consistent with these limits. Recombination lines in the frequency range 100–150 MHz from this gas must therefore become observable with only slightly improved sensitivity.

## 8. Acknowledgements

We thank V. Radhakrishnan, R. Nityananda and G. Srinivasan for useful comments. DB thanks National Council of Educational Research and Training for financial support and Raman Research Institute for extending research facilities.

## References

- Altenhoff, W. J., Downes, D., Pauls, T., Schraml, J. 1978, *Astr. Astrophys. Suppl. Ser.*, **35**, 23.  
 Anantharamaiah, K. R. 1985a, *J. Astrophys. Astr.*, **6**, 177 (Paper I).  
 Anantharamaiah, K. R. 1985b, *J. Astrophys. Astr.*, **6**, 203 (Paper II).  
 Bania, T. M. 1980, *Astrophys. J.*, **242**, 95.  
 Brocklehurst, M., Salem, M. 1977, *Computer Phys. Commun.* **13**, 39.  
 Casse, J. L., Shaver, P. A. 1977, *Astr. Astrophys.*, **61**, 805.  
 Cohen, R. J., Davies, R. D. 1976, *Mon. Not. R. astr. Soc.*, **175**, 1.  
 Cowie, L. L., Songaila, A. 1986, *A. Rev. Astr. Astrophys.*, **24** (in press).  
 del Romero, A., Gómez-González, J. 1981, *Astr. Astrophys.*, **104**, 83.  
 Falgarone, E., Lequeux, J. 1973, *Astr. Astrophys.*, **25**, 253.  
 Field, G. B., Goldsmith, D. W., Habing, H. J. 1969, *Astrophys. J.*, **155**, 149.  
 Gómez-González, J., Guélin, M. 1974, *Astr. Astrophys.*, **32**, 441.  
 Harding, D. S., Harding, A. K. 1982, *Astrophys. J.*, **257**, 603.  
 Hart, L., Pedlar, A. 1980, *Mon. Not. R. astr. Soc.*, **193**, 781.  
 Haslam, C.G.T., Salter, C.J., Stoffel, H., Wilson, W.E. 1982, *Astr. Astrophys. Suppl. Ser.*, **47**, 1.  
 Heiles, C. 1980, *Astrophys. J.*, **235**, 833.  
 Jenkins, E. B. 1984, in *IAU Coll. 81: The Local Interstellar Medium*, Eds Y. Kondo, F. C. Bruhweiler & B. Savage, NASA CP-2345, p. 155.  
 Jenkins, E. B., Meloy, D. A. 1974, *Astrophys. J.*, **193**, L 121.  
 Kesteven, M. J., Pedlar, A. 1977, *Mon. Not. R. astr. Soc.*, **180**, 731.  
 Little, A. G. 1974, in *Galactic Radio Astronomy*, Eds F. J. Kerr & S. C. Simonson, D. Reidel, Dordrecht, p. 491.  
 Lockman, F. J. 1980, *Astrophys. J.*, **241**, 200.  
 Lockman, F. J., Gordon, M. A. 1973, *Astrophys. J.*, **182**, 25.  
 McKee, C. F., Ostriker, J. P. 1977, *Astrophys. J.*, **218**, 148.  
 Oster, L. 1961, *Rev. mod. Phys.*, **33**, 525.  
 Pauls, T., Mezger, P. G., Churchwell, E. 1974, *Astr. Astrophys.*, **34**, 327.  
 Pauls, T., Downes, D., Mezger, P. G., Churchwell, E. 1976, *Astr. Astrophys.*, **46**, 407.  
 Pedlar, A., Davies, R. D., Hart, L., Shaver, P. A. 1978, *Mon. Not. R. astr. Soc.*, **182**, 473.  
 Radhakrishnan, V., Sarma, N. V. G. 1980, *Astr. Astrophys.*, **85**, 249.  
 Rodriguez, L. F., Chaisson, E. J. 1979, *Astrophys. J.*, **228**, 734.  
 Rogerson, J. B., Spitzer, L., Drake, J. F., Dressler, K., Jenkins, E. B., Morton, D. C., York, D. G. 1973, *Astrophys. J.*, **181**, L97.  
 Schwarz, U. J., Ekers, R. D., Goss, W. M. 1982, *Astr. Astrophys.*, **110**, 100.  
 Shaver, P. A. 1975a, *Pramana*, **5**, 1.  
 Shaver, P. A. 1975b, *Astr. Astrophys.*, **43**, 465.  
 Shaver, P. A. 1976, *Astr. Astrophys.*, **49**, 149.  
 Shaver, P. A., Pedlar, A., Davis, R. D. 1976, *Mon. Not. R. astr. Soc.*, **177**, 45.  
 Simonson, S. C., Mader, G. L., 1973, *Astr. Astrophys.*, **27**, 337.  
 Spitzer, L. 1956, *Astrophys. J.*, **124**, 20.  
 Vivekanand, M., Narayan, R. 1982, *J. Astrophys. Astr.*, **3**, 399.  
 York, D.G. 1974, *Astrophys. J.*, **193**, L127.